

SEGMENTATION FOR OBJECT EXTRACTION OF TREES USING MATLAB AND SAGA

Benjamin Bechtel¹, Andre Ringeler¹ & Jürgen Böhner¹

¹Institute of Geography – Section Physical Geography – University of Hamburg, Bundesstr. 55, D-20146 Hamburg (Germany)

Abstract: This paper compares alternative region growing algorithms with respect to their suitability for automated extraction of trees from aerial imagery. Two of the algorithms were especially designed for this purpose and were implemented in MATLAB while the third is an all-round region growing implemented in SAGA. Both were combined with a straightforward radiometric model to evaluate the accuracy and tested with an aerial image showing a pine plantation. Besides that special attention was drawn to the question of portability of algorithms. The simple model was found to be adequate in terms of complexity and performance. Regarding the different segmentation algorithms, the more general method in SAGA seemed less suitable for the sophisticated task of object extraction, since it stresses less emphasis on the geometric condition of the extracted regions. In contrast most objects have certain geometric features like compactness and simply connectedness which already should be utilised in the segmentation step. But wherever model assumptions like these are introduced in an algorithm it should be marked clearly to address the difficulty of portability of algorithms under different conditions. Therefore additional parameters were introduced to the specialised algorithms which were found to be useful to adapt to the given dataset.

1 INTRODUCTION

In the last few decades, the growing importance of Geoinformatics at the interface of Geosciences and Computer Sciences has considerably increased the need for high quality and spatial high resolution geodata. One answer to the problem of how to provide vast amounts of geodata at commensurate scales is the automated extraction of objects from remotely sensed data. Therefore, two knowledge based concepts are utilised: the formalisation of knowledge in order to be processed by computers in model-generation and the application of this knowledge for extraction (HINZ 2003).

Particularly trees are a challenging matter of object extraction given their heterogeneity in appearance and scale which has been addressed by several disciplines (including forestry science, remote sensing, geosciences and computer sciences) for more than two decades. In forestry the main aim is to support forest management and reduce the high costs of conventional forest inventory. Due to the important role of forests in biodiversity, national and international environmental policies require a high demand for environmental monitoring of forest resources.

To date, a wide range of techniques to extract single trees from both, optical (e.g. PINZ 1989, GOUGEON 1995, POLLOCK 1996, BRANDBERG & WALTER 1998, LARSEN & RUDEMO 1997, ERIKSON 2004a) and LIDAR-vector data (HYYPÄ *et al.* 2001, PERSSON 2001, PERSSON *et al.* 2002, HEURICH *et al.* 2004, MORSDORF *et al.* 2004) or a combination of both (STRAUB 2003) have been proposed, all with promising results but mostly limited to simple forest conditions. Most algorithms, designed and optimised for specific datasets, are distinctly less suitable for performing with different data sets or forest conditions.

Moreover the specific preconditions for the application of certain algorithms and the basic assumptions about the image material are not properly defined. Against this background, ERIKSON *et al.* (2006: 1) stated: "It is most likely that none of today's methods are alone able to handle all types of forests. Comparative studies of different segmentation methods with different types of forests are therefore of importance in order to clarify how much a method is reliable with respect to a certain type of forest. This

knowledge can, for instance, be used to build up an expert system which is supposed to be able to extract individual tree crowns in any type of forests". Therefore, both comparative studies evaluating existing algorithms for different conditions and a more conceptual analysis of the problem of "portability of algorithms" are required. Only if the underlying assumptions are explicitly defined, an expert system could select the best available algorithm for any given image. Furthermore existing algorithms should be improved to address a wider range of problems by introducing suitable control parameters.

In this paper several region-growing-algorithms for image segmentation including the SAGA region growing (BÖHNER *et al.* 2006) are tested with a new aerial image scene of a pine plantation in South Africa. For the extraction of the tree hypothesis a very simple but suitable model is introduced.

2 MATERIAL AND METHODS

Study site and data: The analysed dataset is an aerial image of a pine plantation close to Franschhoek in the Western-Cape-Province of South Africa. The scene shows a part of the La Motte Plantation of the South African Forestry Company Limited Company, which is situated north of the Hottentotten nature reserve at about 33.9268°S/19.0664°E. The image was taken in March 2006 with a digital reflex camera from a microlight aircraft in low flight altitude of about 300m. It was georeferenced and pre-processed with the Leica Photogrammetry Suite and has a ground resolution of about 15cm.

The available image is jpeg-compressed but was chosen as an example of lower radiometric quality to test the adaptability of the algorithms. The contrast is rather low and shows an interesting characteristic. In the section LAMOTTE1 shown in Fig. 2 about 8.9% of the pixels in the red channel have less than 15% of the maximum intensity while it are only less than 0.5% of the pixels in the green and blue channel respectively. Since ideally the shadows should be black throughout the spectrum, the path radiance should be little due to the small flight height and the scattering is potentially higher in the red channel (the mean reflectance in the red channel is higher than in the blue channel due to the red soil) it can be concluded that the radiometric sensitivity of the camera is different in the three channels.



Fig. 1: The analysed scene: pine plantation close to Franschhoek, South Africa.

The image shows about 12 year old *Pinus radiata* trees. The stand structure is rather simple since all trees are of cohort age and separated in equal distances. The crowns are quite circular und compact. They have the appearance of a brighter spot (so called blob) but are only partly separated by shadows. Since the sun is directly reflected from the surface, there are also bright soil-blobs in the image, which pose an additional challenge for the extraction. Therefore the utilised model should at least be able to distinguish trees from ground patches.

From the scene two sections were selected. LAMOTTE1 is from the centre, while LAMOTTE2 is from the upper right and geometrically distorted. Both are shown in Fig. 2 together with the according reference regions, which were extracted manually from the aerial image by an operator.

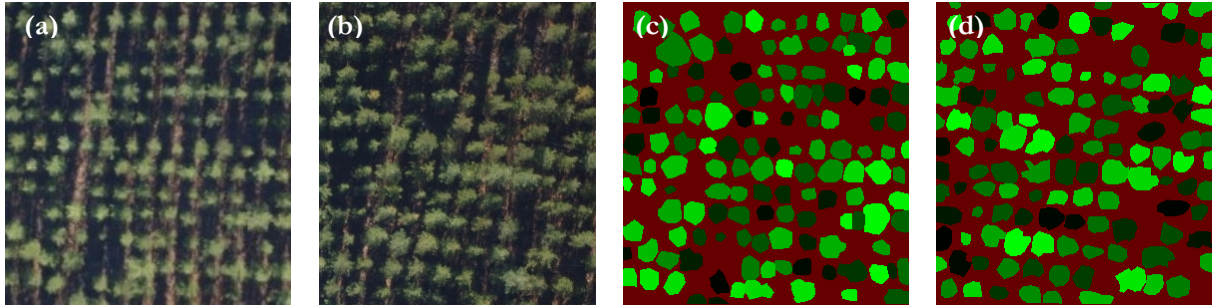


Fig. 2: Sections of the used scene: LAMOTTE1 (a) and LAMOTTE2 (b) and reference regions for LAMOTTE1 (c) and LAMOTTE2 (d).

Strategies in object extraction: Generally two approaches are differentiated in image analysis. Top-down approaches like template matching (POLLOCK 1996, LARSEN & RUDEMO 1997) start at a high level of representation and try to project and decompose a 3-D model into the image. Bottom-up analysis starts by pre-processing the image, finding and grouping features like edges (BRANDBERG & WALTER 1998) or regions (PERSSON *et al.* 2002, STRAUB 2003 and DIEDERSHAGEN *et al.* 2003) and trying to match those with the higher level model in a classification step. Thereby the segmentation of the image and the choice of suitable features are the key tasks, while the classification itself is a standard problem in pattern recognition, covered by a wide range of algorithms.

Region Growing is a class of segmentation procedures in image processing where – starting with single pixels (so called seeds) – image regions are expanded as long as they fulfil a certain homogeneity or similarity criterion, which can contain both radiometric and spatial features. The result is highly dependent of a suitable similarity measure as well as the quality of initial seeds which implies that seed-generation is an important part of the overall segmentation procedure. In the following, three specific region growing algorithms are presented and tested with the above dataset.

Basic Region Growing: The Basic Region Growing (BRG) algorithm is based on the work of ERIKSON (2003, 2004a, ERIKSON & OLOFSSON 2005). Starting from the seeds all neighbour-pixel that meet the similarity-condition expressed in [1] are merged with the adjacent regions:

$$\exp\left(-\frac{1}{2}\left(\frac{(\mathbf{f}_p - \mathbf{f}_s)(\mathbf{f}_p - \mathbf{f}_s)}{\sigma_1} + \frac{(\mathbf{r}_p - \mathbf{r}_s)(\mathbf{r}_p - \mathbf{r}_s)}{\sigma_2}\right)\right) > \alpha \quad [1]$$

where \mathbf{r}_p is the position of the candidate pixel in position-space, \mathbf{f}_p is the position in colour-space and \mathbf{r}_s and \mathbf{f}_s are seed positions in position-space and colour-space respectively. The superscript t indicates vector transposition, σ_1 und σ_2 are variances in colour and position space respectively and α is the threshold for the similarity-criterion. Since the distributions don't need to be normalised α can be chosen freely and is set to 0.15 in ERIKSON & OLOFSSON (2005). For a given threshold the variances can be determined from

formula [1] in the following way: σ_I controls the maximum allowed distance in colour-space. For a maximum distance of 40% of the peak intensity (which is normalised to 1 in a pre-processing step) in each of the three colour channels in the image, the variance is:

$$[2] \quad \sigma_1 = \sqrt{\frac{3 * 0.4^2}{-2 \ln(\alpha)}} = 0.3557$$

Accordingly σ_I controls the maximum spatial distance δ which is the largest crown radius in the case of spherical-shaped crowns:

$$[3] \quad \sigma_2 = \sqrt{\frac{\delta^2}{-2 \ln(\alpha)}}$$

Segmentation via Brownian motion: The segmentation via Brownian motion (BROWNMO) is also based on ERIKSON (2004a) but extended by additional control-parameters. The basic idea is the simulation of the motion of a virtual particle in the image according to the random movement of real particles in liquids or gas. Therefore, starting at the seed point, normalised random vectors are added to the particle's virtual position and the number of visits at every pixel and from every single seed-point is recorded in a Matrix called numPass. Since the particle should preferably not leave the crown, the step distance is modified in the following way: The darker the pixel that would be reached without modification the smaller the step. The position \mathbf{r}_i after i steps is given by:

$$[4] \quad \mathbf{r}_i = \mathbf{r}_{i-1} + w(\mathbf{I}(\mathbf{r}_{i-1} + \mathbf{z}))\mathbf{z}$$

where \mathbf{I} is the image, \mathbf{z} a random vector and w the weight function.

In this algorithm several assumptions about the radiometric properties of trees in the image are drawn, e.g. that trees are brighter than the background, that the centre of the tree is the brightness peak and that there are dark valleys between the trees existing. Each run stops after NUM_STEPS steps and is repeated NUM_RUN times. This was introduced as a new feature to cut the impact of accidentally running into adjacent crowns. The effects of the parameters can be seen in an idealised experiment in a one-dimensional homogenous white image in Fig. 4. The number of runs controls the size of the visited region, the number of steps the certainty of the resulting distribution and therefore the quality of the result. Furthermore the probability density is isotropic which means it is just a function of the distance from the seed point, not of the direction. Consequently it is assumed, that the sought object is circularly shaped and that the seed point represents the centre.

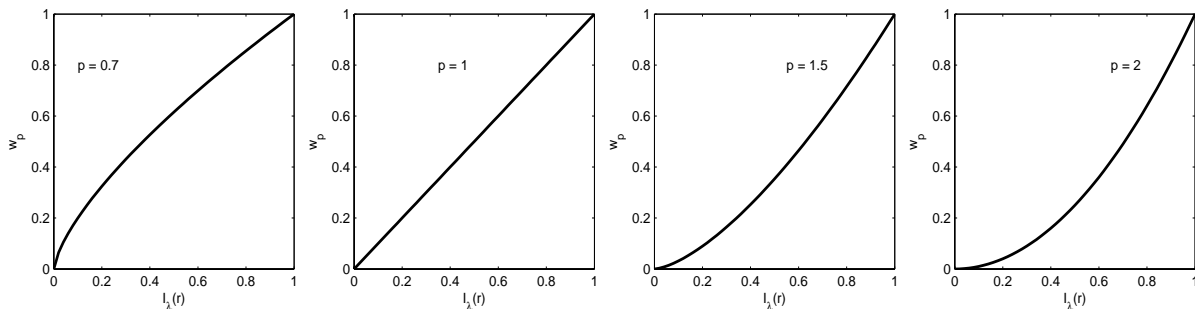


Fig. 3: Weight functions w_p for $p = 0.7, 1, 1.5$ and 2 .

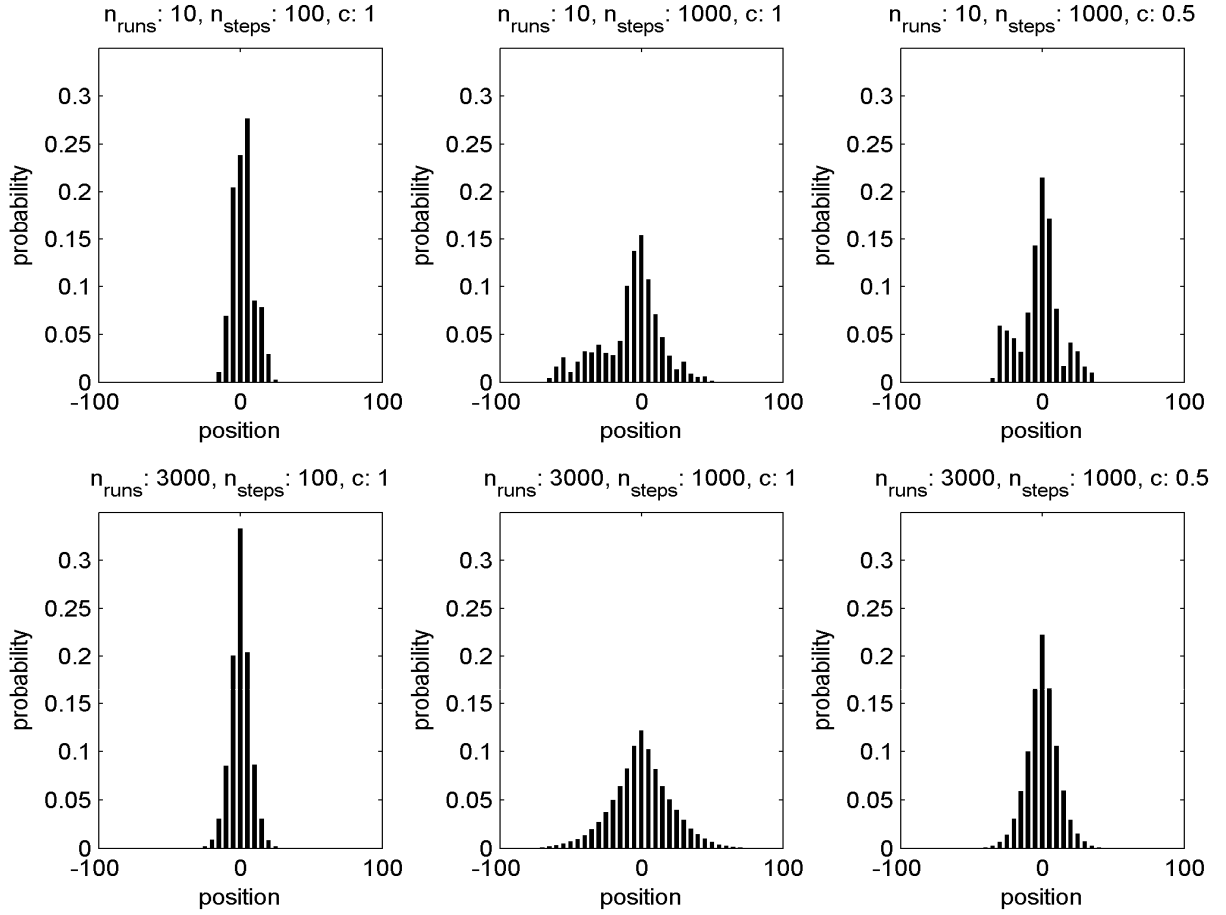


Fig. 4: Relative probabilities of finding a particle at a certain position in an idealised experiment (1D homogenous white image) with different parameter settings. Top: 10 runs, bottom: 3000; Left: 100 steps, middle and right: 1000; left and middle: constant weight factor $c=1$, right: $c=0.5$.

Another way to modify the result in order to increase the portability is the use of different weight functions. For example if due to atmospheric scattering the shadows are not as dark as assumed, a modified weight function could prevent the particle from entering shadow-areas. ERIKSON (2004a) himself uses the grey value of the target pixel (which are normalised to the range $[0..1]$) multiplied by a constant factor c as a weight function:

$$w(\mathbf{I}(\mathbf{r})) = c I_\lambda(\mathbf{r}) \quad [5]$$

Fig. 4 shows the effect of a constant factor of 0.5 at the right side compared to 1 in the middle. But generally any monotonically increasing function of the type:

$$w : \mathbf{I}(\mathbf{r}) \mapsto [0 : 1] \quad [6]$$

would also be suitable as a weight function. Several different weight functions were tested, e.g. linear combinations of different colour channels:

$$w(\mathbf{I}(\mathbf{r})) = \frac{1}{n} \sum_{\lambda=1}^n a_\lambda I_\lambda(\mathbf{r}), \text{ with } \sum_{\lambda} a_\lambda = 1 \quad [7]$$

(which includes the arithmetic mean of the colour channels red, green and blue for $a_R = a_G = a_B = 1/3$). Furthermore different powers of the functions were tested. For a single channel the according weight function is:

$$[8] \quad w_p(\mathbf{I}(\mathbf{r})) = (I_\lambda(\mathbf{r}))^p$$

The effect is shown in Fig. 3: for a higher power it becomes less likely, that the particle runs into darker areas, but at the same time the mean step width (as well as the segmented area) becomes smaller similar to the constant factor in Fig. 4.

The actual region growing is performed in a second step after the generation of numPass. The region of every seed is initialised with the largest circle of pixels that have been visited in the numPass image. Then all neighbouring pixels (according to 4-neighbourhood) are administrated in a list. The list is sorted and processed in order of the numPass values so that the pixel with the most visits is added to the region first. Afterwards the list is updated with the new neighbour pixels which are not member of a region so far and have a sufficient numPass value. The algorithm terminates when the candidate list is empty.

SAGA Seeded Region Growing (SRG): For segmentation of multispectral sensor data in feature space (also property space) a fast seeded simultaneous region growing algorithm is implemented in SAGA. The starting seeds for the algorithm can be defined manually, or determined automatically by the SAGA maximum representativeness analysis module as described in BÖHNER *et al.* (2006).

The recursive region growing process is presented schematically in Fig. 5. Starting with the seeds as an initial set of clusters, a list of border pixels $B_1 \dots B_n$ containing their 4-neighbours, the pixel values in all dimensions of feature space $x_1 \dots x_n$ as well as their adjoining clusters is built. For every border point B_i and every adjacent cluster the maximum Euclidean distance in feature space to any other pixel in the cluster d_i is computed and the list is sorted by increasing distances. This complete linkage strategy guarantees spectrally homogenous clusters and avoids the risk of centroid linking, where the clusters radiometric features can alter during processing. In every step the first pixel in the list is associated with the cluster; the boundary pixel list is updated and resorted. For a more detailed description see BÖHNER *et al.* (2006).

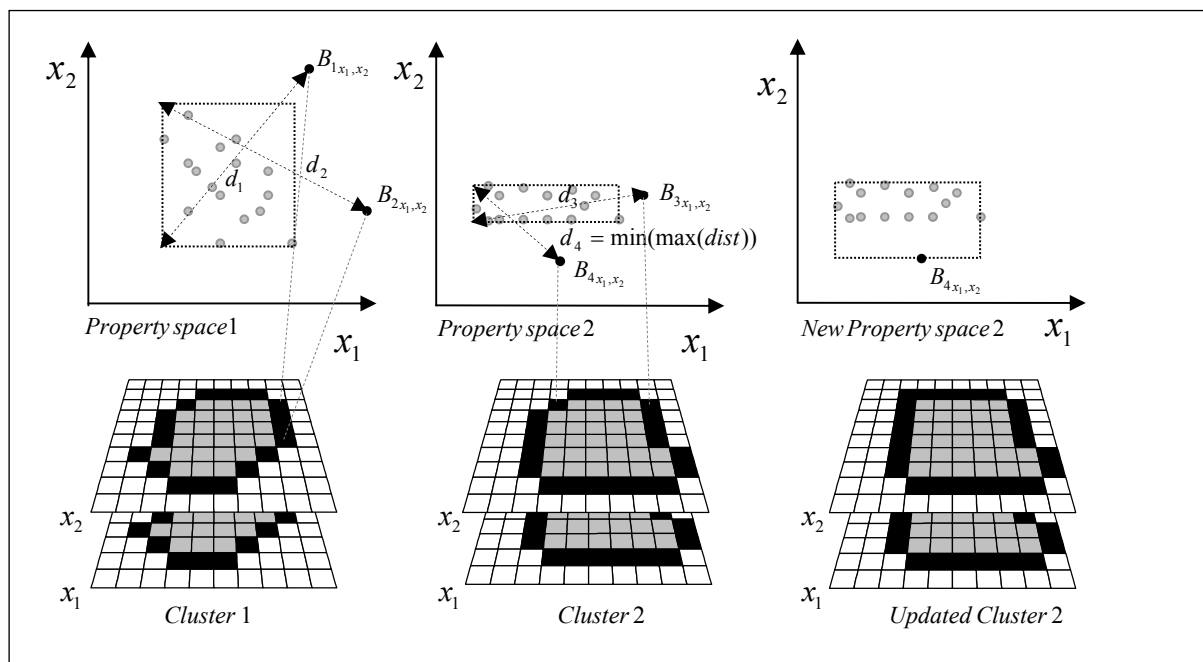


Fig. 5: Schematic description of the linkage in SAGA Seeded Region Growing.

Since a region merging algorithm for post processing is not implemented yet, the results of the region growing process tend to over-segmentation. While the algorithm is designed to produce compact regions in feature space it doesn't necessarily produce compact regions in position space, which can be connected in any possible way.

Evaluation: to compare the results certain regions are selected as a valid tree hypothesis in the following way. Using the module `bbFeatureExtraction`, in a first step, several features of the regions are extracted, including the geometric features AREA, SOLIDITY, CIRCLENESS and RADIUS, which refer to the whole region and the radiometric features, which are mean values of all (BRIGHT and DOA) or a subselection (BOUND_BRIGHT) of the pixels of a region (for detailed description of the features see BECHTEL 2007: 90).

The model should be appropriate for the complexness of the given situation which means basically it must be able to distinguish crowns from ground patches and shadows. Since the geometric features are partly determined by the selected segmentation algorithms (particularly in case of BRG and BROWNMO), radiometric features seem most suitable. The degree of artificiality (DOA – like NDVI with green and red channel) is a measure, to distinguish between ground patches and crowns whilst the brightness is considered, to eliminate shadow-regions. Consequently, $[DOA > 0 \ \&\& \ BRIGHT > \text{mean}(BRIGHT)]$ forms a straightforward model with *a priori* fixed decision boundaries and is implemented as 'DOA & Bright' in the module `bbHypoSelect`.

Secondly the accuracy is assessed by comparing the selected regions with the reference polygons. For matching, an overlap factor according to STRAUB & HEIPKE (2004) is defined:

$$OF_{AB} = \frac{A \cap B}{\min(|A|, |B|)} \quad [9]$$

An $OF > 0.5$ is considered as a match and written to a `matchlist`. In the case of several overlaps fulfilling the criterion for a single region, the one with the biggest overlap is chosen.

3 RESULTS

Fig. 6 shows the result of BRG on LAMOTTE1. The seeds in the first figure were generated with a special technique giving an estimated size of the corresponding tree (for details see BECHTEL 2007, ERIKSON 2004b) which is used to initialise the variance in [3] if the parameter `AUTO_TREE_SIZE` is set. Consequently the segmented regions in the second figure are allowed to differ in size. Beside trees single ground patches are segmented, which are excluded by the hypothesis selection in the third figure. This is possible because the BRG segmentation doesn't presume high radiometric intensity but just relative homogeneity. The last figure shows the result of the matching with the reference data. The completeness is 86% and the correctness 98%, but all false positives are half trees at the image boundary which means it is even better. The area of the trees was underestimated systematically and is 74% on average. Since the darker areas at the crowns' boundaries are not part of the segmented regions in some cases, the ratio of the convex hull of the segmented regions to the reference was chosen as a second measure for accuracy and is 83% on average for this run. The mean positional error is 2.2 pixels corresponding to 32cm, which can be assessed as good.

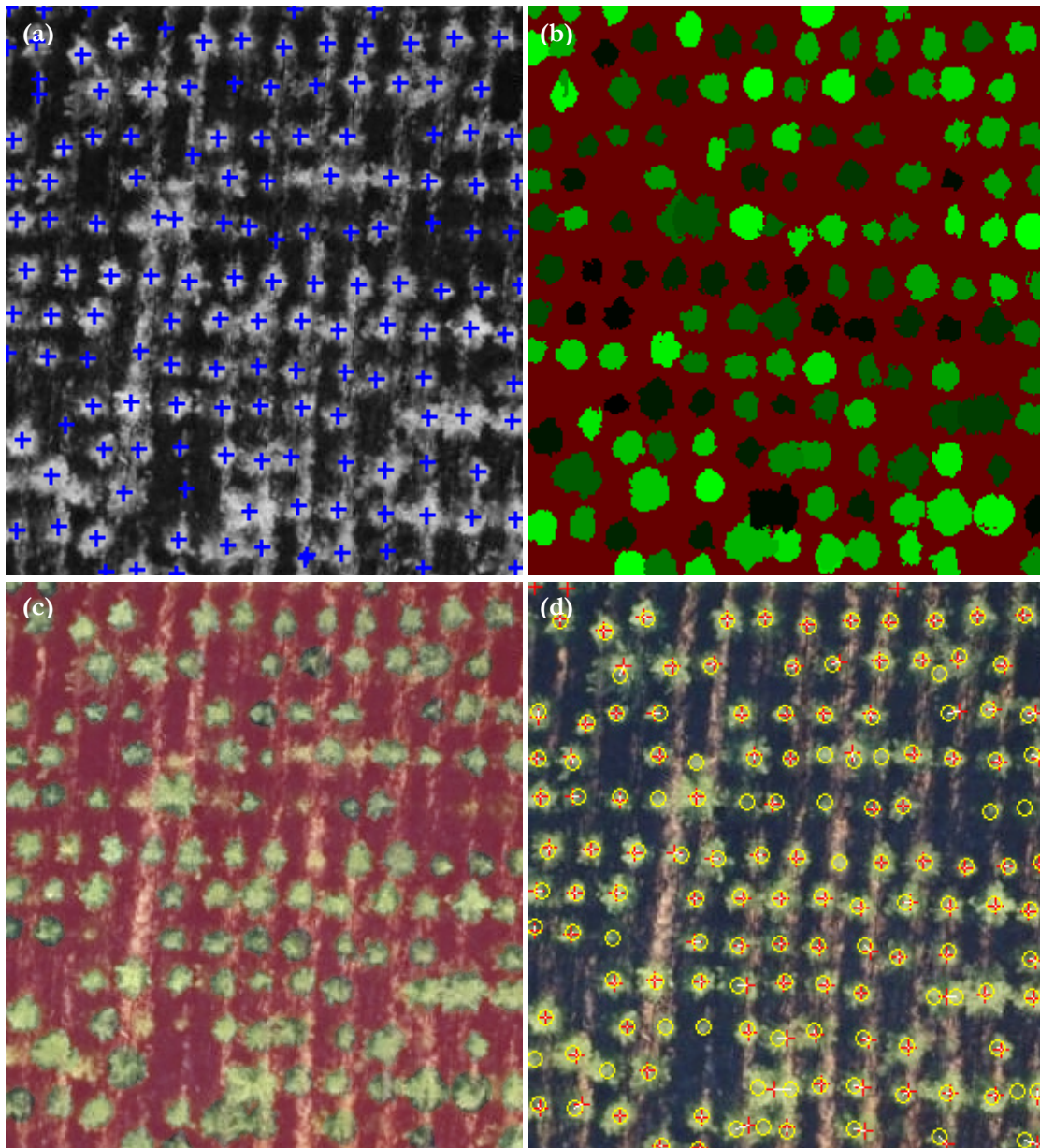


Fig. 6: Results of BRG with LAMOTTE1: seed-points (a), segmentation result (b), selected tree hypothesis (c) and matching with reference trees (d); red crosses indicate extracted trees, yellow circles indicate reference trees and the white lines indicate the matches.

Fig. 7 shows the result of BROWNMO with LAMOTTE2. As weight function the mean of the three colour channels with a weight power of 1.5 was chosen. The segmented regions in the first figure show a different characteristic since the virtual particle accidentally ran into adjacent ground patches. In the second figure it is recognisable that the model mistakenly discarded some actual trees due to their radiometric properties. Some of them might be infected by wood warps and thus have altered their colour but partly it might also be owed to the radiometric quality of the image, since all those regions have a degree of artificiality of less than zero. The third figure shows the matching results and the last plot the ratio between extracted and actual size (red crosses) and the same for the convex hull (green crosses) respectively. The completeness of the run is 84% and the correctness is 96%. The mean positional error is 38cm and the area is 80% of the reference on average.

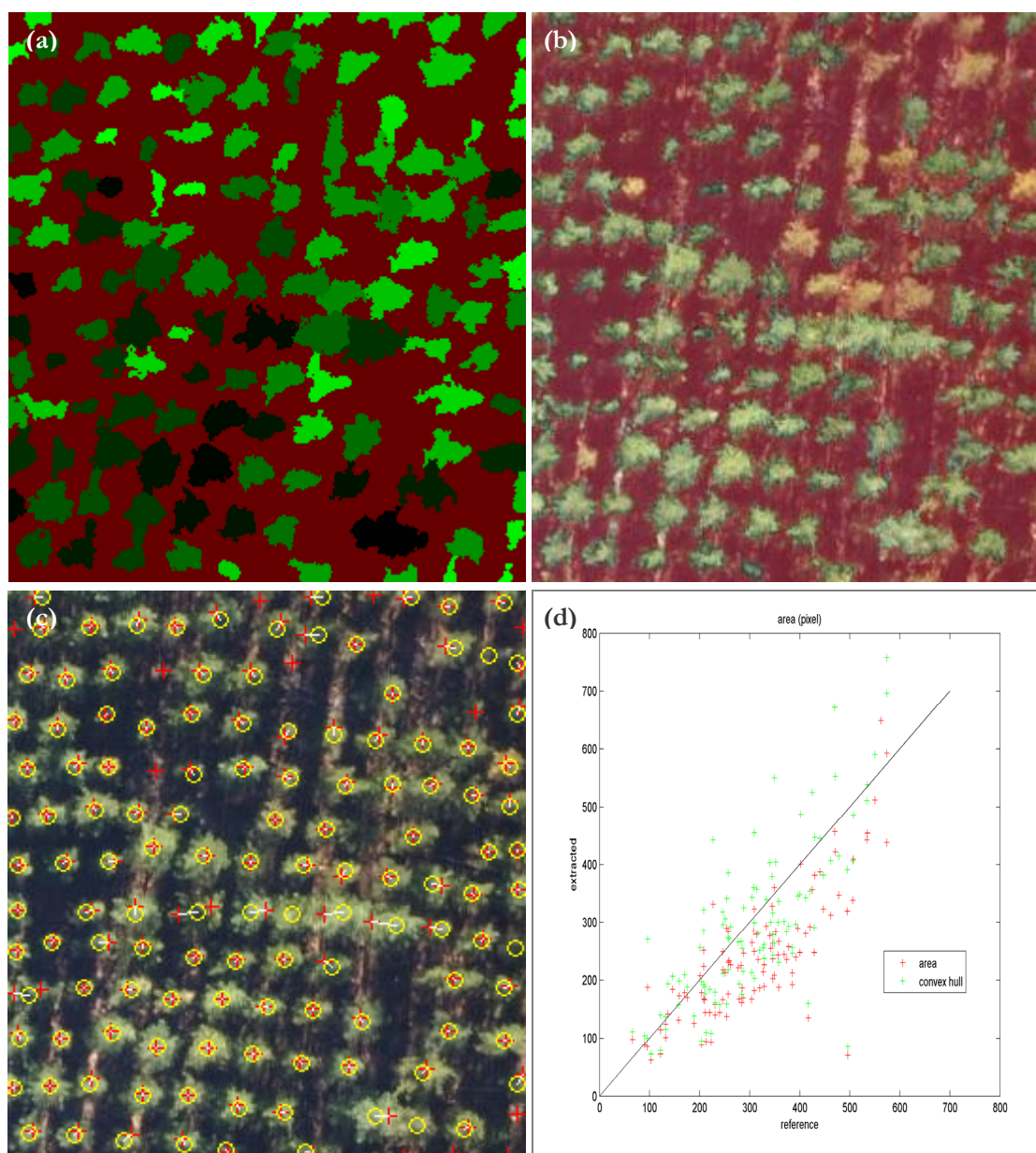


Fig. 7: Results of BROWNMO with LAMOTTE2: segmented regions (a), selected tree hypothesis (b), matching with reference trees (c), comparison of extracted and reference area of the matched regions (d).

The results of SRG with LAMOTTE2 in Fig. 8 illustrate, that the applied radiometric model is also very suitable for hypothesis selection with the complete segmentation of SRG, even though the extracted regions have rather specific radiometric than geometric conditions. The third figure reveals a certain over-segmentation of the image. Especially the crown borders tend to be segmented into “midtone” regions, which mostly comprise several crowns like in the highlighted example. This is a result from the high emphasis on radiometric homogeneity while the only geometric requirement is 4-neighbour connection and leads to outliers in the matching of the extracted regions.

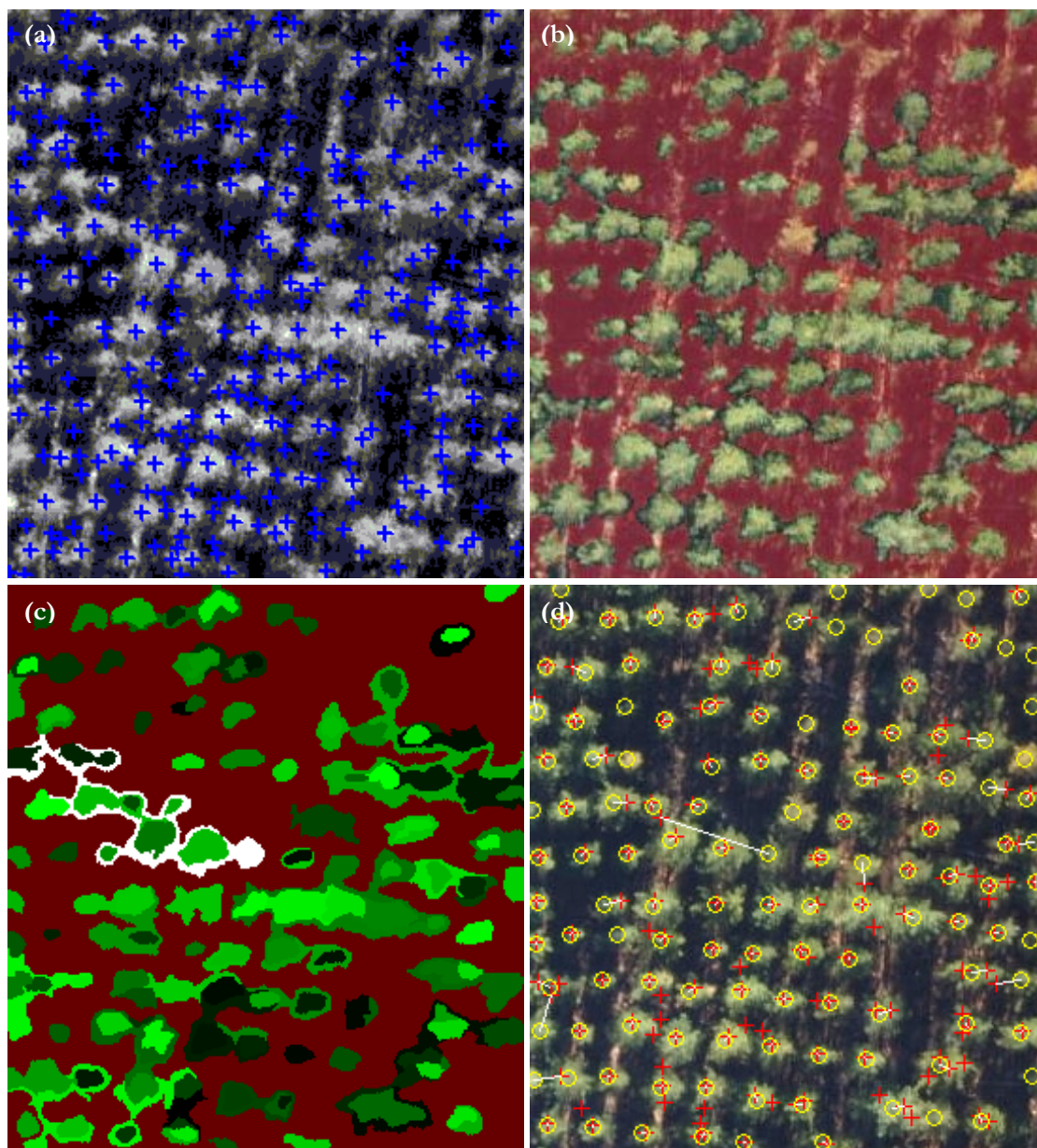


Fig. 8: Results of SRG with LAMOTTE2: seed points (a), selected tree hypothesis as masked image (b) and corresponding regions (c), matching (d).

4 DISCUSSION AND CONCLUSIONS

For BRG and BROWNMO the completeness is between 80 and 90% and the correctness is 95% or even more, comparable with better values achieved in other studies for similar forest stands (STRAUB 2003), which is a good result considering the simplicity of the utilised model. The accuracy of the extracted parameters (especially position and crown area), however, requires a more differentiated assessment.

With BRG the crown area was systematically underestimated, but according to ERIKSON “it is important that the segmentation result preserves the contour of the tree crown since it is used for classifying [...]” (2004b: 471). Particularly shaded parts of the crown are not added to the segment but exactly this feature can be used to discriminate different species. Furthermore for most forestry applications the relevant size is the crown diameter instead of the crown area which should be less affected by the shadowing effect. Anyway it has to be stated that the reference data was manually extracted from the image and may therefore underestimate the crown size as well or even completely hide small shaded trees (see PERSSON *et al.* 2002).

Tab. 1: Accuracy of the extraction result for the datasets LAMOTTE1 (LM1) and LAMOTTE2 (LM2) with different segmentation algorithms and the simple model ‘DOA & Bright’; wf = ‘G’: only green channel, ‘RGB_mean’: all colour channels, wp: power of weight function.

	BRG		BROWNMO				SRG	
Dataset	LM1	LM2	LM1	LM1	LM2	LM2	LM1	LM2
Run identifier	BRG1	BRG2	BM1	BM2	BM3	BM4	SRG1	SRG2
Parameters	AUTO_SIZE	AUTO_SIZE	wf:'G'; wp: 1.5	wf:'RGB_mean'; wp: 1.5	wf:'RGB_mean'; wp: 1.5	wf:'RGB_mean'; wp: 2		
Model	DOA & Bright	DOA & Bright	DOA & Bright	DOA & Bright	DOA & Bright	DOA & Bright	DOA & Bright	DOA & Bright
Completeness (%)	86	87	83	81	84	87	88	84
Correctness (%)	98	98	96	95	96	96	69	69
Mean positional error (m)	0.32	0.35	0.34	0.35	0.38	0.41	0.47	0.58
Ratio extracted area / reference region (%)	74	72	100	95	80	51	63	72
Ratio convex complement / Reference (%)	83	79	121	117	99	63	82	120

For BROWNMO the estimated area seems to be more accurate, but this is partly since the virtual particles mistakenly ran into ground patches. This assumption is stressed by the fact that the mean OF is lower for BROWNMO than for BRG (89% for BM1 compared to 93% for BRG1). BM4 was included to show that the completeness and correctness, which are rather dependent from the seed points, are quite robust against the chosen power of weight function parameter, whilst the size of the extracted crowns, instead, is very sensitive to the weight function parameter. With additional runs it was examined whether different weight functions are a suitable parameter to control segmentation output. It could be shown, that higher powers at the weight function produce brighter and more homogenous regions. Since higher powers also lead to smaller regions, this is partly an effect of the texture-specific semi variance, but it still was found useful to adapt to the poor radiometric quality of the given image. In contrast the use of weight functions with different colour channels did not derive any additional benefit.

Though SRG performs well the result shows that for the complex task of object extraction more specialised algorithms which indirectly comprehend model-knowledge are preferable. In particular for the purpose of object extraction more emphasis should be aspired on the compactness and simple connectedness of the extracted regions since most objects tend to have those characteristics. As aforesaid, the crowns are partly decomposed into several regions which mostly show a circular characteristic. Accordingly, the radiometric homogeneity appears to be weighted heavier than the compactness of the region – another model feature, since it usually can be assumed, that trees are compact and simply connected. The over-segmentation results in a high completeness and a little correctness. For the given run (SRG2) 143 regions are selected as hypothesis but after removing double matches (especially two regions matching with one reference tree) only 105 are left. Accordingly the area ratio is rather low. In contrast fringe regions like the highlighted in Fig. 8 form outliers, resulting in a huge ratio of the convex hull which is obviously no suitable measure for non- simply connected regions.

The mean positional area is small (about 30-40cm for BRG and BROWNMO and a bit higher for SRG due to outliers) which is partly an effect of the rather strict matching rules. If the underlying concept of matching identity was loosened, the positional error would increase but the error of omission would decrease. Against this background and in order to make SAGA a more valuable tool for object extraction, we propose to introduce more sophisticated segmentation algorithms including parameters for the compactness in position space.

REFERENCES

- BECHTEL, B. (2007): Objektextraktion von Bäumen aus Luftbildern. Vergleich und Steuerung von Segmentierungsverfahren zur Vorbereitung eines Expertensystems. – Diploma thesis at the University of Hamburg.
- BÖHNER, J., SELIGE, T. & A. RINGELER (2006): Image segmentation using representativeness analysis and region growing. – In: BÖHNER, J. MCCLOY, K.R. & J. STROBL (Eds.): Göttinger Geographische Abhandlungen 115: 29-38.
- BRANDBERG, T. & F. WALTER (1998): Automated delineation of individual tree crowns in high spatial resolution aerial images by multiple-scale analysis. – *Machine Vision and Applications* 11: 64-73.
- DIEDERSHAGEN, O., KOCH, B. & H. WEINACKER (2003): Automatic Estimation Of Forest Inventory Parameters Based On Lidar, Multi-Spectral And FOGIS Data. – *Proceedings Optical 3-D Measurement Techniques VI II*: 259-269.
- ERIKSON, M. & K. OLOFSSON (2005): Comparison of three individual tree crown detection methods. – In: *Machine Vision and Applications* 16(4): 258-265.
- ERIKSON, M. (2003): Segmentation of individual tree crowns in colour aerial photographs using region growing supported by fuzzy rules. – *Canadian Journal of Forest Research* 33: 1557-1563.
- ERIKSON, M. (2004a): Segmentation and Classification of Individual Tree Crowns in High Spatial Resolution Aerial Images. – Uppsala.
- ERIKSON, M. (2004b): Species classification of individually segmented tree crowns in high-resolution aerial images using radiometric and morphologic image measures. – *Remote Sensing of Env.* 91: 469-477.
- ERIKSON, M., PERRIN, G., DESCOMBES, X. & J. ZERUBIA (2006): A comparative study of three methods for identifying individual tree crowns in aerial images covering different types of forests. – In: *Proc. Int. Society for Photogrammetry and Remote Sensing (ISPRS)*, Marne La Vallee, France, July 2006.
- GOUGEON, F.A. (1995): A crown-following approach to the automatic delineation of individual tree crowns in high resolution aerial images. – *Canadian Journal of Remote Sensing* 21(3): 274-284.
- HEURICH, M., PERSSON, Å., HOLMGREN, J. & E. KENNEL (2004): Detecting and measuring individual trees with laser scanning in mixed mountain forest of central Europe using an algorithm developed for Swedish boreal forest conditions. – *International Archives of Photogrammetry, Remote Sensing and Spatial Information Sciences* 36 - 8/W2.
- HINZ, S. (2003): Automatische Extraktion urbaner Straßennetze aus Luftbildern. – München.
- HYYPÄ, J., SCHARDT, M., HAGGRÉN, H., KOCH, B., LOHR, U., PAANANEN, R., SCHERRER, H.U., LUUKKONEN, H., ZIEGLER, M., HYYPÄ, H., PYYSALO, U., FRIEDLÄNDER, H., UUTTERA, J., WAGNER, S., INKINEN, M., WIMMER, A., KUKKO, A., AHOKAS, E. & M. KARJALAINEN (2001): HIGH SCAN: The first European-wide Attempt to Derive Single-Tree information from Laserscanner Data. – *The Photogrammetric Journal of Finland* 2(17): 58-68.
- LARSEN, M. & M. RUDEMO (1997): Estimation of Tree Positions from Aerial Photos. – In: LINDEBERG, T. (Ed.): *Proceedings of the 1997 Swedish Symposium on Image Analysis*, pp. 130-134.
- MORS DORF, F., MEIER, E., ALLGÖWER, B. & D. NÜESCH (2004): Cluster-Analyse von LIDAR-Vektordaten zur Erfassung geometrischer Eigenschaften von einzelnen Bäumen. – *Photogrammetrie, Fernerkundung, Geoinformation* 4/2004: 259-268.
- PERSSON, A. (2001): Extraction of Individual Trees using Laser Radar Data. – Linköping.
- PERSSON, A., HOLMGREN J. & U. SÖDERMAN (2002): Detecting and Measuring Individual Trees Using an Airborne Laser Scanner. – *Photogrammetric Engineering & Remote Sensing* 9 (68): 925-932.
- PINZ, A. (1989): Final results of the Vision Expert System VES: finding trees in aerial Photographs. – In: PINZ, A. (Ed.): *Wissensbasierte Mustererkennung*. Wien.
- POLLOCK, R.J. (1996): The Automatic recognition of Individual trees in Aerial Images of Forests based on a Synthetic Tree Crown Image Model. – Vancouver.
- STRAUB, B.M. & C. HEIPKE (2004): Concepts for Internal and External Evaluation of Automatically Delineated Tree Tops. – In: *IntArchPhRS XXXVI 8/W2*, pp. 62-65. Freiburg.
- STRAUB, B.M. (2003): Automatische Extraktion von Bäumen aus Fernerkundungsdaten. – In: *Wiss. Arbeiten, Fachrichtung Vermessungswesen* 249. Hannover.